Mechanically actuated variable flux IPMSM for EV and HEV applications

I.Urquhart[1], D.Tanaka[2], R. Owen[3], Z.Q.Zhu[3], J.B Wang[3], D.A Stone[3]

[1]Nissan Motor Manufacture Co., Ltd. (UK)

[2]Nissan Motor Co., Ltd (Japan)

[3] Dept. of Electronic & Electrical Engineering, University of Sheffield, UK

Email: Iain.Urquhart@ntc-europe.co.uk

Abstract

The current trend in production EVs/HEVs is to use interior permanent magnet synchronous motors (IPMSM) as the means of providing power to the vehicle drive train.   The efficiency of these machines can be extremely high (>95%) although this typically occurs in a relatively narrow range in the middle of the machine speed-torque curve.   This is a concern for automotive applications as vehicles operate across the full range of speeds and torques; typical urban drive cycles operate in the low speed/torque region where efficiencies can drop to below 80%.   Clearly there is a mismatch between the region of high efficiency of the machine and the region of highest operation duty of EVs/HEVs.   This paper presents a method of expanding the peak efficiency region of the machine by introducing a method for adjusting the permanent magnet flux linkage utilising a mechanism that short circuits the flux at the end caps of the rotor using solid steel plates. These plates are operated such that they can switch between open and closed positions depending on the demand on the machine allowing the flux linkage to be varied.   Analysis shows that by applying the plates to short the flux in the rotor the flux linkage in low torque/high speed applications is lowered whilst reducing the need for high flux weakening currents in the d-axis. This reduces current consumption, improving the power factor and therefore increases the overall efficiency of the machine.   The performance of the system is verified using a proof of concept IPMSM.

1. Introduction

Permanent magnet machines are well suited to EV and HEV applications given their favourable torque and power density characteristics which are well summarised in a large number of reviews on the subject [1]-[5].   Generally, permanent magnet machines can generate high levels of torque output when they are designed with a high permanent magnet flux density in the rotor. This is because the cross product of the magnetic flux and the current is roughly proportional to the torque output, thus the greater the magnetic flux density the lower the current required to generate a given torque.

However, a consequence of increasing flux density is that such machines have a higher back EMF constant which is a linear product of the flux density and the speed of the rotor. In order to limit the voltage level of the system below its input DC voltage, a control technique called flux weakening [6] can be utilised where current is applied such that some of the flux generated by the coils suppresses the flux from the permanent magnets. The additional current required to implement this control technique within the flux weakening region results in less efficient torque generation. In addition the high flux density from the permanent magnets combined with the high frequency of the flux within the core at high rotor speeds creates large eddy currents and associated iron loss within the rotor and stator cores. The therefore motors with high permanent magnet flux densities tend to have higher efficiency in the low speed/high torque regions but reduced efficiency in the high speed/low torque region where the flux weakening current is prominent [7]. For automotive applications, in which vehicles operate across a wide range of speeds and torques, the motor is designed such that its maximum efficiency is in the mid-torque/speed range of the machine speed-torque curve. However, this is a concern for operation of vehicles in the real world because a typical urban drive cycle requires the machine to operate in the low speed/torque region where efficiencies can drop to 80%. Fig.1 illustrates an example of the mismatch between the region of high efficiency of the machine and the region of highest operation duty of EVs/HEVs.
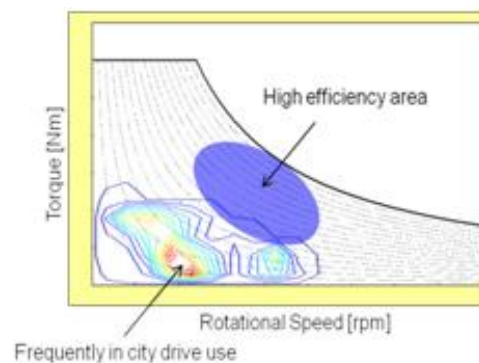

Figure 1: High efficiency area Vs high operation duty

2. Overview of the Concept

The initial stages of the study involved a detailed investigation of a large number of different variable flux permanent magnet (VFPM) motors as summarised in a previous paper [8]. The outcome of the study found the optimum solution to be a mechanical variable flux machine utilising a short circuit mechanism at the end caps of the rotor [9]. The mechanism employs plates made of magnetic steel which are operated such that they switch between an open position, where the plates are apart from the end cap and a closed position where the plates sit in contact with the rotor. Actuation is dependent on the driving demands of the machine allowing the flux linkage to be varied.

2.1 Variable flux concept – influence of design parameters

As previously discussed the principle of the variable flux machine is to adjust the flux linkage, ψ_a, such that it is maximised for low speed-high torque applications and minimised for high speed-low torque applications. Fig. 2 illustrates the concept.
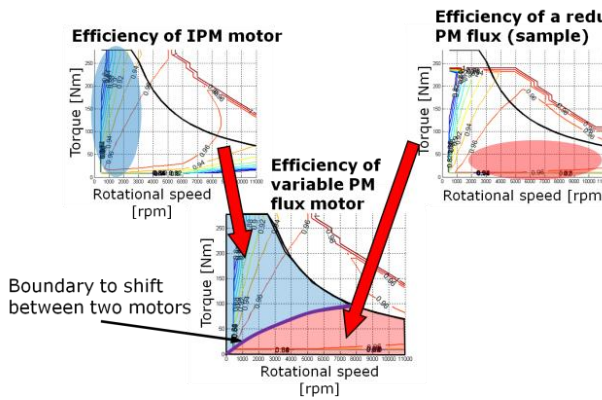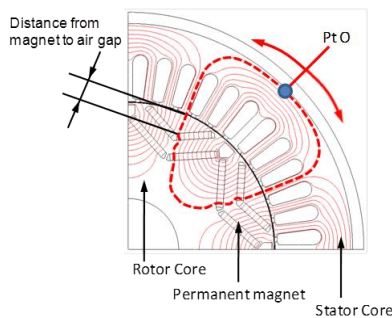
Figure 2: Variable flux concept illustration

From fig 2 it can be seen that the mechanism merges the characteristics of two machines into one, above a given speed/torque boundary the mechanism allows maximum flux linkage to enable efficient high torque capabilities, below the boundary the mechanism switches the machine to minimum flux condition allowing for increased efficiency in the high speed/low torque region.
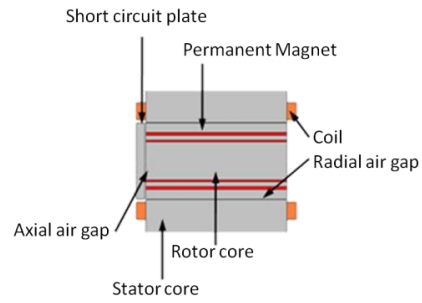
In order to understand the capability of the mechanism to reduce the flux, analysis of the relevant parameters that influence the ability of the mechanism to adjust the flux level need to be understood.

To reduce development time simplified 2D analytical models combined with 2D FEA were utilised to build a picture of which features can be optimised to maximise the effect of mechanism.

Fig. 3 shows a simplified model of the motor cut in the axial direction along the d-axis.

(a) ¼ Radial section of motor

(b) Axial section of simplified model from Pt0

Figure 3: Simplified model of motor

The parameters initially investigated were:

- The effects of stack factor of the rotor core lamination
- Layout of the buried permanent magnets (single layer, dual layer etc)
- Distance from the magnets to the radial air gap (depth in rotor)

The iron cores of both the rotor and the stator are made up of thin laminated plates which are stacked together. Between each plate is a thin layer of insulation which provides electrical isolation and is essential to reducing iron loss within the core. Addition of the insulation results in the total length of iron being shorter than the total length of the rotor core. The ratio between these two lengths is the stack factor, and can be summarised by equation (1) below.

$$Stack\ factor = \frac{\sum T_{iron}}{L_{total}} \times 100\% \quad (1)$$

Where T_{iron} is the thickness of iron in each plate and L_{total} is the total stack length.

Derivation of the amount of flux reduced is obtained using equation (2) below. This gives a ratio, α, of flux short circuited by the mechanism in each case.

$$\alpha = \frac{\lambda_{norm} - \lambda_{sc}}{\lambda_{norm}} \quad (2)$$

Where λ_{norm} is the flux linkage without the short circuit plates and λ_{sc} is the flux linkage with the

plates attached.   With the short circuit plate fully attached to the end cap of the rotor, α is calculated. As previously indicated two different magnet layouts are investigated, single and double layer magnets.   Fig 5 below shows the difference in topology.
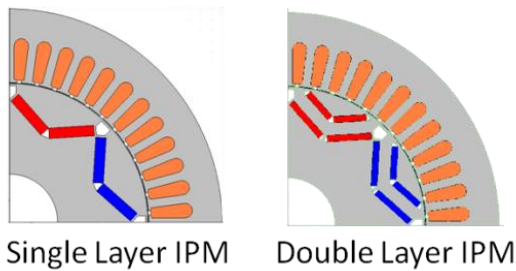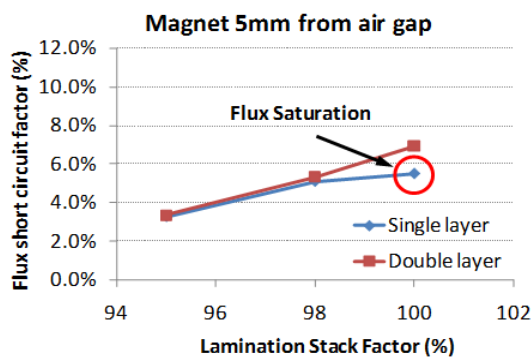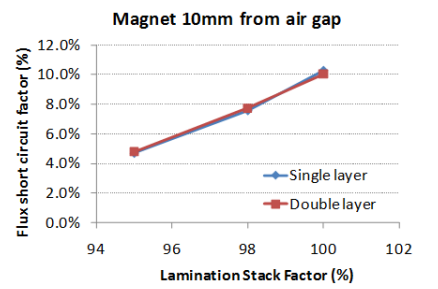

Figure 5: Single layer and double layer topologies

Single layer topologies tend to have lower magnet volumes and less leakage leading to slightly higher magnet efficiency than dual layer topologies whereas dual layer topologies allow for better control of the flux distribution across the air gap leading to a reduction in loss making high harmonics in the back EMF waveform.

Both these topologies are investigated with respect to the lamination stack factor and the distance of the magnet from the rotor-stator air gap; this is calculated for one end of the rotor shaft only.   Fig. 6 shows the results.

(a) Ratio α, with magnet 5mm from airgap

(b) Ratio α, with magnet 10mm from airgap

Figure 6: Calculation result of α with varying stack factor, magnet layers and distance to air gap

From the results the following observations can be made:

- Stack factor plays a critical role in the effectiveness of the short circuit plate to reduce the net flux linkage in the airgap
- Increasing the depth of the magnets in the rotor improves the performance of the short circuit plate
- Double layer magnet layout reduces risk of flux saturation in the rotor, particularly at high stack factors

In addition to understanding the maximum level of flux reduction the effect of moving the short circuit plate away from the end cap must be understood. Assuming a dual layer magnet layout with the magnet buried 10mm from the radial air gap the plate is moved from 0mm to 2.5mm in an axial direction away from the rotor.   This is shown in fig.6.
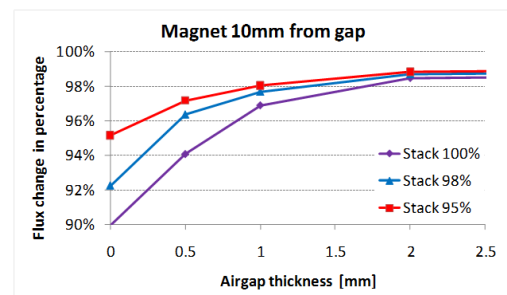

Figure 6: Axial flux leakage versus air gap between short circuit plate and rotor

Clearly as the air gap increases the reluctance increases and therefore less flux will bridge the gap between the rotor and the short circuit plate. Fig 6 also clearly shows the stack factor has a large influence on the effectiveness of the mechanism. Given laminated steel 0.35mm thick a typical stack factor of 98% would mean that the mechanism can only reduce the flux linkage to the stator by 7.5%. The short circuit mechanism relies on flux being able to move orthogonally to the plane of each lamination plate. However, between each lamination plate is a small layer of insulation, representing a reluctance equivalent to a small air gap. These high reluctance 'air gaps' stack up in series as one moves further into the rotor core, thus magnetic flux from deep in the core will observe a high reluctance path preventing any axial movement. Introducing a short circuit mechanism to each side of the rotor doubles the effectiveness of the system which means the total reduction in flux would be 15%.

2.2 Optimising the machine design

In theory the stack factor of lamination plates can be high, up to 98.3% but in practice the standard methods used to align and strengthen the stack mean the stack factor typically reduces to 95%. This is because standard forming processes such as cleating are imperfect and cannot provide strong enough bond to achieve the 98% stack factor that is required to achieve the highest reduction in flux. Alternative methods such as adhesive bonding will not achieve the required stack factor as the addition of the adhesive to the plate increases the thickness of the insulation layer, reducing the overall stack factor. A good method is welding. On the stator the lamination plates are typically welded along the external axial length of the stator structure [10], such that it is outside the main magnetic circuit allowing a strong mechanical bond between the plates without any negative effects on the performance of the machine. Applying the same method to the rotor is counter-intuitive; the process of welding creates a series of short circuits along the active length of the core directly into the main magnetic circuit which results in large eddy currents and associated losses.
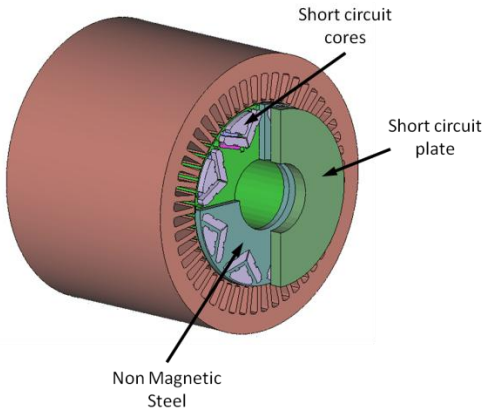
If, however, the inner bore of the rotor is welded, then a strong mechanical link can be formed and much like the outer diameter of the stator back-iron this region of the iron core lies outside the magnetic circuit so the risk of eddy currents is minimised.

The limitation of this solution is that a specialist laser welding tool is required to fit into the inner bore of the rotor; whilst not a major technical issue this will result in increased tooling costs. The action of welding will also induce splay, where the clamp force on the inner diameter causes the plates to separate in the axial direction towards the outer diameter of the rotor. To counter the splay, the plates are compressed prior to magnet insertion to ensure that any splay is minimised and the increased stack factor is maintained during the setting period of the adhesive. When the core is inserted onto the rotor, end caps shrunk fit onto the shaft can provide a constant clamp force to remove any splay.
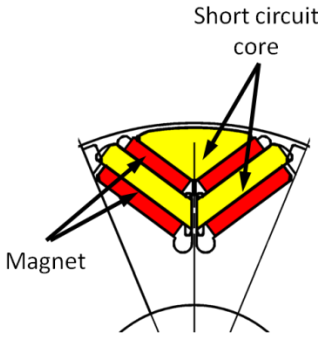
The requirement for end caps presents a key design issue; the 2D models described thus far work on the assumption that the short circuit plates sit directly against the magnets in the minimum flux condition. Whilst this works well for studying

the magnetic circuit, in practical terms this is unrealistic. As described above the core requires a constant clamp force both to hold the rotor on the shaft and to ensure the core material does not splay. In addition the neodymium magnets used are sintered parts and as such inherently brittle making them prone to damage under the high stresses induced when the short circuit plates snap onto the end of the rotor. A high strength material must be placed between the magnet and the short circuit plate to mitigate this risk.

Standard machine design utilises plates made of non-magnetic materials such as stainless steel which are typically shrunk-fit to the shaft such that they provide strength and limit any axial flux leakage. This presents a problem; using non-magnetic material such as stainless steel has the same effect as putting a large air gap between the ends of the magnets and the short circuit plates. This would negate the benefit of the mechanism and prevent further development of the concept. To circumvent this concern the end caps must be designed such that the optimal flux flow between the magnets can occur when the short circuit plates are fully engaged, but limit flux leakage when the plates are moved apart from the rotor. Fig 7 shows the initial design.

(b) Short circuit core layout relative to magnets

Figure 7: Initial end plate design

The initial simulation results of the design are shown in table 2 below.

Table 2 – Effect of applying initial end cap design

	Base Motor	Variable flux V1	
Magnetic Flux (mWb)	76.13	67.36	-11.5%

From the results of the initial design it can be seen that the flux linkage with the short circuit plates fully attached reduces by 11.5% over the base condition. This is somewhat short of the original estimations where the short circuit plate was attached to the rotor laminations. 3D Analysis of the flux flow in the design highlights an imbalance in the flux distribution within the short circuit plates. Fig 8 shows high concentrations of flux saturating materials in the upper magnet layers and an under utilisation of the lower region of the short circuit plates such that the net axial flux linkage is limited.
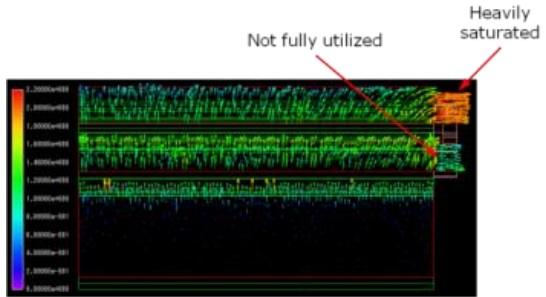

(a) Overview of end plate layout

Figure 8: Axial flux saturation in end cap

The problem is caused by the 'V' shape of the

double layer magnet concentrating the flux into the upper iron core, creating a heavily saturated upper level whilst not utilising the material available in the lower level. To counteract this concern the 'V' shape of the dual layer magnet design was modified such that surface area of the inserts interfacing with the end plates is increased to reduce the saturation in the upper region and more evenly distribute the flux density. The process of adjusting this fundamental item requires care as a balance between maintaining the maximum flux linkage to the stator and ability of the rotor core to minimise stress concentrations must be found. Fig 9 shows the resultant design.
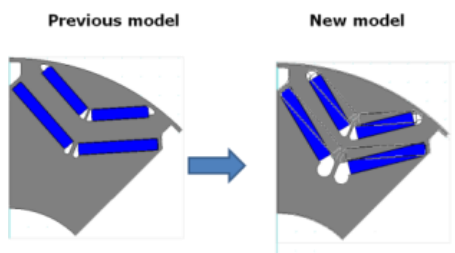

Figure 9: 'V' shape topology optimisation result

Table 3: Results of magnet 'V' shape optimisation

	Base Motor	Variable flux V2	
Magnetic Flux (mWb)	76.27	64.85	-15.0%

Table 3 indicates the new layout of the magnets reduces the saturation within the short circuit mechanism by better distribution of the flux such that a reduction of 15% in the flux reduction can be obtained. Further improvements in the design can be achieved by optimising the geometry of the solid steel inserts in the end cap assembly. The plates are modified such that the contact area between the magnets and the short circuit plates is maximised.
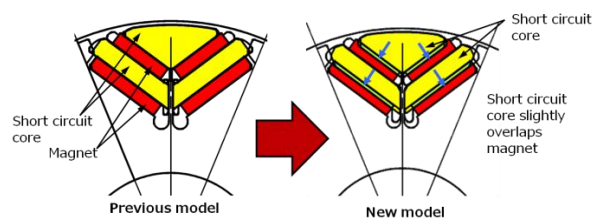

Figure 10: Optimisation of short circuit inserts

Fig 10 shows the plates are enlarged such the upper layer and lower layer of magnets are slightly overlapped by the respective upper and lower inserts. This removes reluctance due to any minor air gap between the inserts and the magnets created by tolerance concerns etc. Table 4 shows the effects of the final design.

Table 4: Result of optimised short circuit cores

	Base Motor	Variable flux V3	
Magnetic Flux (mWb)	76.35	64.34	-15.7%

The results show a 15.7% reduction in flux with the plates fully engaged.

The final design point is to determine the maximum air gap required between the rotor end cap and the short circuit plates, the goals are to minimise that the flux leakage as far as possible for the maximum flux condition but not so far as to add complications to the actuation mechanism. To determine the optimum distance the axial air gaps at each end of the rotor were increased in steps of 1mm from 0mm (short circuit position) to 10mm. The result is shown in fig 14 below.
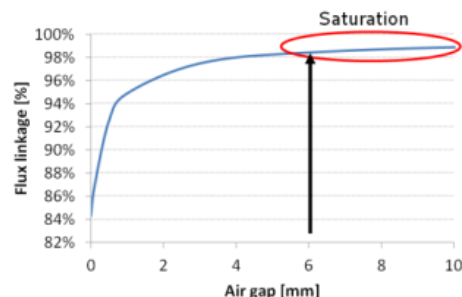

Figure 11: Flux linkage change VS axial air gap

The graph in fig 11 shows the flux linkage changing non-linearly as the plate is moved away from the rotor end cap; this is a reflection of the inverse square law of the magnetic field strength. Once the plate moves past 6mm the gain in moving the plate further becomes negligible as the change in flux is effectively saturate. Note the flux linkage will never reach 100% due to small amounts of flux leakage in the end caps. Fig 12 below shows the final machine design.
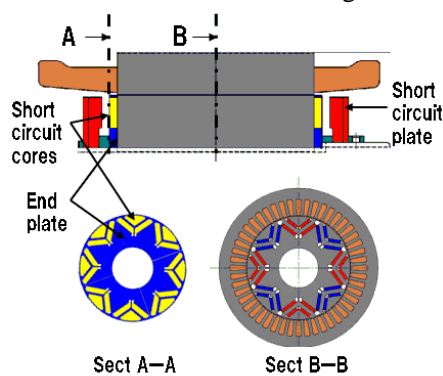

Figure 12: Final motor structure

3 Verifying the Performance

Following the development of the machine using 2D CAE techniques the performance of the machine was verified utilising 3D FEA tools.

Three versions of the developed machine were modelled;

- Base motor (no mechanism),
- Variable flux motor with the plates 6mm from the rotor (max flux condition),
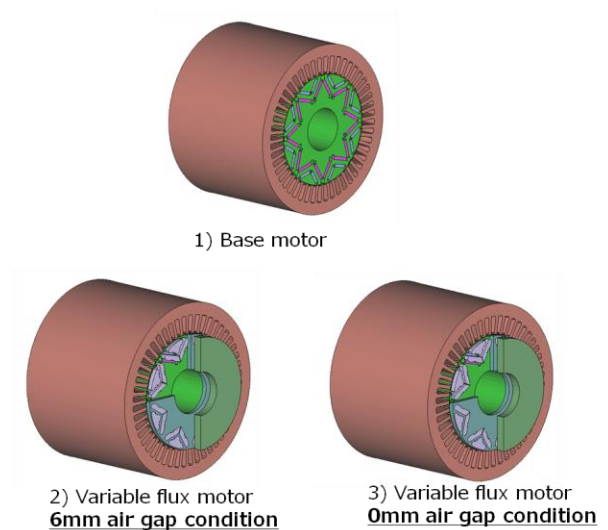- Variable flux motor with plates 0mm from the rotor (min flux condition). Fig 13 below shows the three settings.

Figure 13: Three motor settings

3.1 Base Motor *vs.* 6mm air gap condition

The first check is to verify that the variable flux machine achieves the same performance as the base machine in the maximum flux condition. Table 5 shows the difference in motor constant at maximum torque.

Table 5: Comparison of motor constants between base motor and variable flux motor @6mm

Simulation	Magnet flux Ψ_a [mWb]	Ld [mH]	Lq [mH]
Base motor 3D	89.7	0.11	0.20
Variable flux	**88.5**	**0.12**	**0.21**
Difference	**98.7%**	**108.1%**	**102.9%**

As can be seen there is a 1.3% reduction in Ψ_a whilst d-axis inductance has increased 8.1% due to the leakage inductance in the short circuit cores.

3.2 Base Motor *vs.* 0mm air gap condition

Setting the machine to minimum flux condition allows a comparison of the machine constant to be drawn between the base machine and the reduced flux machine. Table 6 shows the motor constant at maximum torque.

Table 6: Comparison of motor constants between base motor and variable flux motor @0mm

Simulation	Magnet flux Ψa [mWb]	Ld [mH]	Lq [mH]
Base motor 3D	89.7	0.11	0.20
Variable flux	77.2	0.12	0.21
Difference	**86.0%**	**111.6%**	**105.4%**

The results show a reduction in flux of 14% between the base motor and the variable flux machine, this is slightly short of the original 15% alluded to in the more simplistic analysis but full 3D analysis of the machine means aspects such as iron loss and flux leakage are taken better modelled thus the effective flux can drop by a few %, as indicated in the results.

3.3 Effect of reduced flux at high speed

A key item is to contrast the performance of the variable flux mechanism in the high speed/low torque with the base motor to verify the initial claims of improve performance hold true. Table 7 shows results of the motor running at a load of 50Nm at 9000rpm.

Table 7: Base Motor VS VFIPMSM at high speed

50Nm@9000rpm		Base motor	Variable flux	Ratio
Copper loss	[kw]	1.33	0.64	-52.0%
Iron loss	[kw]	2.42	1.95	-19.2%
Total loss	[kw]	3.75	2.60	**-30.9%**

Copper loss is reduced by 52%, indicating the significant benefits of reducing the flux weakening current over the base machine and the reduced flux density in the iron reduces the iron loss by 19.2% leading to a 30.9% improvement over the base machine during high speed operation. This clearly shows the benefit of the mechanism as the reduction in loss expands the efficiency band, as shown in fig 14.
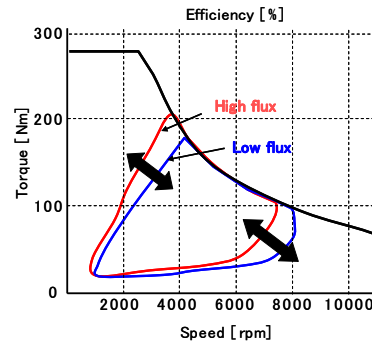

Figure 14: Expansion of peak efficiency region

4. Prototype Machine Testing

The 3D FEA results confirmed the mechanism could provide the required level of flux reduction. Whilst this is encouraging even modern FEA packages cannot fully replicate the complexities and variable tolerance stack-ups that exist in fabricated machines. Thus to fully validate the real-world performance of the machine a full scale prototype machine was fabricated.

Similar to the 3D FEA results, 3 rotor variants were tested; a base rotor, rotor with end plates fixed to 6mm from rotor end cap and a 0mm setting with the short circuit plate fully engaged to the rotor. Fig 18 below shows the three rotor variants.
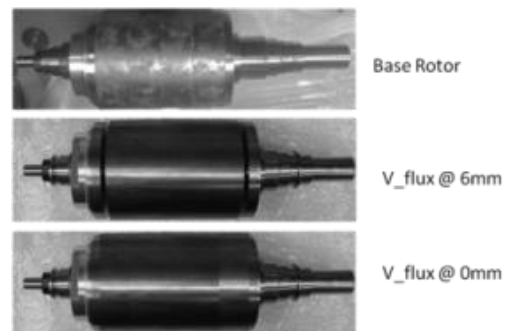

Figure 18: Fabricate rotor variants.

The base rotor differs from the variable flux rotor by having blank stainless steel plates as end caps, reducing the risk of flux leakage between the magnet tips at the outer edges of the rotor. The

machine is mounted to a dynamometer, fig 19, and the back EMF of each rotor at 1200rpm is measured.
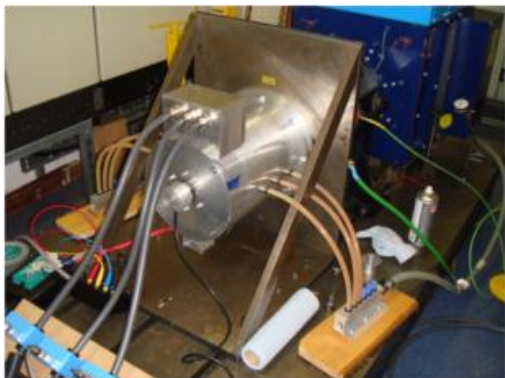

Figure19: Prototype machine under test

4.1 Back EMF comparison of base motor FEA results and measured prototype

The initial check is to identify any differences between the back EMF profile and amplitude. Fig 20 below shows the results.
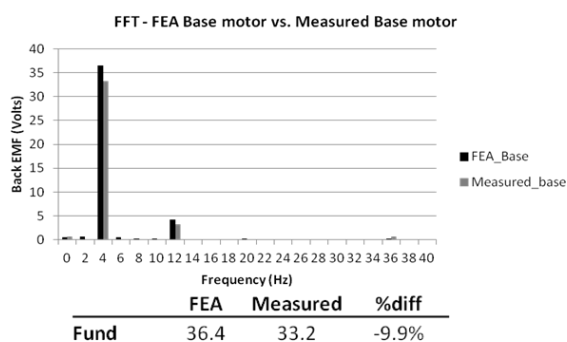

Figure 20: FFT – measured vs. FEA base motor

From the results it can be seen that there is 9.9% reduction in the peak voltage and by extension the flux linkage between the prototype motor and the 3D FEA results. A study into this loss was undertaken to try and find the source of the discrepancy. The study found two sources of loss:

- Rotor and stator core material grade
- Additional air gaps in the magnetic circuit due to requirement for additional slot size for magnet adhesive and tolerance stack

up in the machine

The FEA model was modified to try and replicate the results, 2D modelling was used to accelerate the study. The results are shown in table 8.

Table 8: Identified loss factors in the prototype

Component	Change Item	Contribution
Core Magnetic Steel	FEA = Nippon Steel 35H210 Prototype = M250-35A	2.5%
Magnet slot Width	FEA = 7mm (direct contact w/core) Prototype = 7.2mm (allow adhesive)	6.7%
	Total:	9.2%

The study accounts for 9.2% of the lost flux, the remaining ~0.7% can most likely be derived from tolerance in the main air gap and tolerance stack up effects within the inserted windings in the slots.

4.2 Back EMF comparison of measured Base motor and measured variable flux rotor with short circuit plates set to 6mm

Following the comparison between the FEA and the prototype base motors the back EMF between the base rotor and the variable flux machine at maximum flux setting is evaluated. The results are shown in fig 21 below.
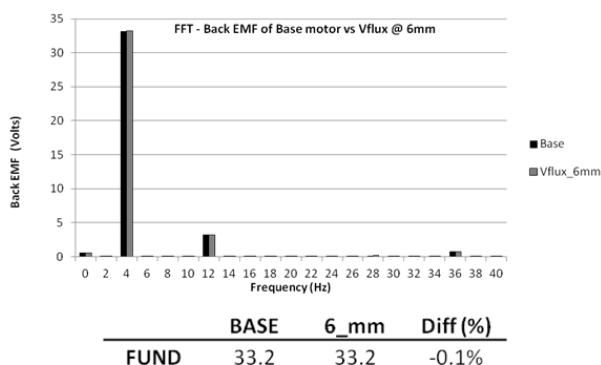

Figure 21: FFT results of Base motor and variable flux machine @ 6mm

The measurement shows a 0.1% difference in flux between the measured base rotor and the variable flux rotor at maximum flux setting. This shows that the prototype variable flux machine can achieve the same performance as the base machine.

4.3 Back EMF comparison of measured variable flux rotor with short circuit plates set to 6mm and 0mm

The final, and most important, comparison is between the variable flux rotor set to minimum and maximum flux conditions.   The results are shown in fig 22 below.

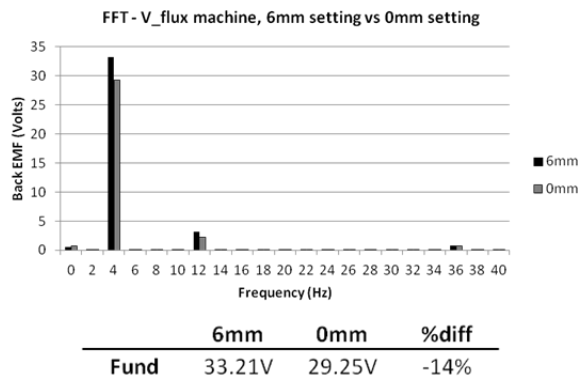|	6mm	0mm	%diff
Fund	33.21V	29.25V	-14%

Figure 22: FFT showing difference in BEMF between 6mm and 0mm settings

The results show that the flux drop between the maximum and minimum flux setting achieves a 14% reduction in flux.   Thus despite the drop in flux linkage between the 3D FEA model and the physical prototype, the short circuit mechanism has been shown to vary the flux as predicted.

5. Conclusion

This paper provided the highlights of a novel machine topology developed to expand the efficiency band of a IPMSM for EV and HEV applications such that it could be used to reduce current consumption and extend the range of the vehicle over a given drive cycle.   A concept providing the best cost/benefit balance was developed and optimised using 2D analytical methodologies and verified initially with 3D FEA then using a fabricated prototype machine.   The resultant machine achieved a satisfactory level, 14%, of flux control by means of mechanical actuation of the short circuit plates, which is expected to improve the efficiency within the high speed region by approximately 30%. .

References

[1] C. C. Chan, "The state of the art of electric, hybrid, and fuel cell vehicles," *Proceedings of the IEEE,* vol. 95, no. 4, pp. 704-718, 2007.

[2] I. Husain, Electric and Hybrid Vehicles – Design Fundamental. Boca Raton: FL: CRC, 2003.

[3] Z. Q. Zhu and D. Howe, "Electrical machines and drives for electric, hybrid, and fuel cell vehicles," *Proceedings of the IEEE*, vol. 95, no. 4, pp. 746-765, 2007.

[4] M. Zeraoulia, M. E. H. Benbouzid, and D. Diallo, "Electric motor drive selection issues for HEV propulsion systems: a comparative study," *IEEE Trans. Veh. Technol.*, vol. 55, no. 6, pp. 1756-1764, 2006.

[5] A. M. El-Refaie, "Motors/generators for traction propulsion applications: a review," in *IEMDC2011*, 2011, pp. 490-497.

[6] Mukhtar Ahmad, "High Performance AC Drives Modelling, Analysis and Control", ISBN 978-3-642-13149-3, Springer,   P.116

[7] Z.Q Zhu, Y.S Chen, D.Howe, "Maximising the flux-weakening capability of PM brushless AC machines and drives", Proceedings of the IPEMC 2000, pp. 552-557 vol 2

[8] R.Owen, Z.Q. Zhu, J.B. Wang, D. A. Stone, I. Urquhart, "Review of Variable-flux Permanent Magnet Machines", International Conference on

Electrical Machines and Systems (ICEMS) 2011

[9] Lei Ma, Masayuki Sanada, Shigeo Morimoto, Yoji Takeda, "Advantages of IMPSM with Adjustable PM Armature Flux Linkage in Efficiency Improvement and Operating Range Extension", PCC Osaka, 2002

[10] J.R. Hendershot jr and TJE Miller, "Design of Brushless permanent magnet motors", ISBN 1-881855-03-1,Magna physics publications, 3-27 to 3-29

Authors

Iain Urquhart received a Bsc (Hons) degree in Artificial Intelligence and Robotics at the Robert Gordon University in Aberdeen in 2004. He Joined the Nissan Graduate scheme in 2004 and worked in Chassis mechatronics design for 6 years, responsible for ABS/ESP, EPAS and TPMS on B and C platform vehicles for the European market. He joined the Nissan Europe Advanced Engineering group in 2009 and was seconded to The University of Sheffield in 2010 to work on EV/HEV drive train research until present

Daiki Tanaka received a B.Eng. degree in mechanical and aerospace engineering from the University of California Davis, Davis, U.S.A., in 2001. He joined Nissan Motor Co. Ltd., Nissan Research Center in 2002 and worked in the research project for CVT for 3 years, responsible for the development and evaluation of novel control algorithm of CVT. He joined the electric machine and power electronics research group from 2005 and has developed novel electric machines and drives until present.

Z.Q. Zhu received the B.Eng. and M.Sc. degrees from Zhejiang University, Hangzhou, China, in 1982 and 1984, respectively, and Ph.D. degree from the University of Sheffield, Sheffield, U.K., in 1991, all in electrical and electronic engineering.
Since 1988, he has been with the University of Sheffield, where he is currently Professor of electrical machines and control systems, Head of the Electrical Machines and Drives Research Group, and Academic Director of Sheffield Siemens Wind Power Research Centre. His current major research interests include design and control of permanent magnet brushless machines and drives for applications ranging from automotive to renewable energy.

Richard L. Owen received a PhD degree and M.Eng. degree in electrical engineering from The University of Sheffield, Sheffield, U.K., in 2011 and 2005 respectively, Subsequently he has worked as a Research Associate at the university

of Sheffield and currently he works for Siemens Wind Power as an electromagnetic design engineer. His research interests include design and analysis of permanent-magnet brushless electrical machines for various

David A. Stone received a B.Eng. degree in electronic engineering from The University of Sheffield, Sheffield, U.K., in 1984 and Ph.D. degree from the University of Liverpool, Liverpool, U.K., in 1989. He returned to The University of Sheffield as a member of the Academic Staff and is currently Professor of Power Electronics and Machine Drive Systems. His current research interests are in novel high efficiency power electronic converters, electric and hybrid electric vehicles, management of electrochemical energy storage systems, grid interfaced storage systems and novel lamp ballasts for low-pressure fluorescent lamps.

Jiabin Wang (SM'03) received the B.Eng. and M.Eng degrees in electrical and electronic engineeringfrom Jiangsu University of Science and Technology, Zhenjiang, China, in 1982 and 1986, respectively, and the Ph.D. degree in electrical and electronic engineering from the University of East London, London, U.K., in 1996. He is currently a Professor of electrical engineering with the University of Sheffield, Sheffield,
U.K. From 1986 to 1991, he was with the Department of Electrical Engineering, Jiangsu University of Science and Technology, where he was appointed Lecturer in 1987 and Associated Professor in 1990. He was a Postdoctoral Research Associate with the University of Sheffield, Sheffield, U.K., from 1996 to 1997 and a Senior Lecturer with the University of East London from 1998 to 2001. His research interests include motion control of electromagnetic devices and their associated drives in applications ranging from automotive to household appliances and the aerospace sector.